Optics Letters

Continuous-wave modulation of a femtosecond oscillator using coherent molecules

D. C. Gold, J. T. Karpel, E. A. Mueller, and D. D. Yavuz*

Department of Physics, 1150 University Avenue, University of Wisconsin at Madison, Madison, Wisconsin 53706, USA
**Corresponding author: yavuz@wisc.edu*

Received 27 November 2017; revised 16 January 2018; accepted 22 January 2018; posted 22 January 2018 (Doc. ID 314247); published 21 February 2018

We describe a new method to broaden the frequency spectrum of a femtosecond oscillator in the continuous-wave (CW) domain. The method relies on modulating the femtosecond laser using four-wave mixing inside a Raman-based optical modulator. We prepare the modulator by placing deuterium molecules inside a high-finesse cavity and driving their fundamental vibrational transition using intense pump and Stokes lasers that are locked to the cavity modes. With the molecules prepared, any laser within the optical region of the spectrum can pass through the system and be modulated in a single pass. This constitutes a CW optical modulator at a frequency of 90 THz with a steady-state single-pass efficiency of $\sim 10^{-6}$ and transient (10 μs-time-scale) single-pass efficiency of $\sim 10^{-4}$. Using our modulator, we broaden the initial Ti:sapphire spectrum centered at 800 nm and produce upshifted and downshifted sidebands centered at wavelengths of 650 nm and 1.04 μm, respectively.

OCIS codes: (190.5650) Raman effect; (290.5910) Scattering, stimulated Raman; (140.3550) Lasers, Raman.

https://doi.org/10.1364/OL.43.001003

Over the last two decades, the invention of and developments in femtosecond lasers have had a big impact on a diverse range of scientific fields, including biological imaging, nanotechnology, and ultrafast spectroscopy [1,2]. Viewed in the time domain, these lasers produce ultrashort pulses that can be used to probe electronic, vibrational, and rotational dynamics at femtosecond time scales. Equally important, viewed in the frequency domain, these lasers enable bridging the microwave and optical frequency standards, since they can generate frequency components covering a wide spectral range (frequency combs). Femtosecond lasers typically produce ∼100 fs-long pulses with spectral bandwidths of a few tens of nanometers. A critical development in the evolution of these lasers was the discovery of methods to broaden their frequency spectrum, which has typically been done using self-phase modulation inside a photonic crystal fiber [3,4]. Using such broadening, an octave-wide spectrum can be produced that allows $f-2f$ spectroscopy and locking of the carrier–envelope phase (CEP) of the comb [2].

In this Letter, we describe a new method to broaden the frequency spectrum of a femtosecond laser oscillator. As we discuss below, the method relies on continuous-wave (CW) optical modulation of the femtosecond oscillator at a rate of 90 terahertz (THz) using Raman-based four-wave mixing. We prepare the optical modulator by driving deuterium (D_2) molecules to a highly coherent vibrational state using intense CW pump and Stokes laser beams inside a high-finesse cavity. Once coherent vibrations are established, we can send any carrier laser through the cavity and produce frequency downshifted (Stokes) and upshifted (anti-Stokes) sidebands. The carrier beam does not need to be resonant with the cavity: the modulation is produced in a single pass. In particular, a femtosecond Ti:sapphire laser oscillator whose spectrum is centered at 800 nm is frequency modulated to produce upshifted and downshifted sidebands centered at wavelengths of 650 nm and 1.04 μm, respectively. The steady-state single-pass efficiency of our modulator is $\sim 10^{-6}$, and transient (10 μs-time-scale) single-pass efficiency is $\sim 10^{-4}$ (the efficiency is the ratio of the generated frequency upshifted sideband power to the incident carrier power).

There are key advantages to using molecular modulation to broaden the frequency spectrum of a femtosecond laser compared to other techniques. With the molecules prepared, the modulation efficiency is constant regardless of the intensity of the carrier beam, and, as a result, femtosecond lasers with arbitrarily low average powers can, in principle, be modulated. Furthermore, due to the low operation pressure of the molecular gas, minimal unwanted dispersion is introduced to the produced broad spectrum. Because of these advantages, one important application of our approach is to ultrafast waveform synthesis. The modulated output is much wider than the initial Ti:sapphire spectrum, with the capability to produce shorter pulses and more complex waveforms. If the modulation efficiency can be increased, multiple-modulation orders with frequencies of the form $\nu_0 + q\nu_M$ (where q is an integer, ν_0 is the carrier frequency, and ν_M is the modulation frequency) may be produced. Such a device may then form the basis for a true arbitrary optical waveform generator with a coherent spectrum covering infrared, visible, and ultraviolet spectral regions. Another application is to precision spectroscopy and optical clocks. Using recently developed techniques, the absolute frequency of the modulator ν_M can be set to a specific value with a

very high precision [2]. As a result, if a stabilized frequency comb is used, the generated sideband frequencies will also be known to very high precision. This may, e.g., allow the construction of optical clocks in different regions of the spectrum or the generation of a broad absolute frequency reference with components covering much of the optical region.

Our experiment builds on a large body of prior work, most importantly by Imasaka and coworkers on two-color stimulated Raman scattering [5,6], by the Harris and Hakuta groups on molecular modulation [7–10], and by Carlsten and colleagues on CW Raman generation inside high-finesse cavities [11,12]. Kung and colleagues have demonstrated the synthesis of non-sinusoidal waveforms using molecular modulation [13], and other recent advances using this technique are listed in Refs. [14–17]. Broadening the spectrum of a femtosecond laser using molecules was first proposed by Kien *et al.* [18], and was later experimentally demonstrated using Q-switched pulsed lasers by Marangos and coworkers [19].

The main ingredients of our experimental setup are similar to our recent experiments [20,21] with the addition of a femtosecond Ti:sapphire oscillator to the system. Figure 1 shows a simplified schematic of the experiment, which is performed inside a cavity with a high finesse both at the pump (1.064 μm) and at the vibrational Stokes (1.56 μm) wavelengths. The high-finesse cavity is placed inside a vacuum chamber that we fill with molecular D_2. The reflectivities of the mirrors at the pump and the Stokes wavelengths are 0.9992, and one of the mirrors is mounted on a piezo-electric transducer to allow for slight adjustments of the cavity length. The mirrors have a radius-of-curvature of 50 cm, and the cavity length is 27 cm, producing a mode radius of 400 μm at the focus. To produce the desired high-power pump laser beam, we start with an external cavity diode laser (ECDL) at a wavelength of 1.064 μm. The ECDL is custom built with an optical power of 20 mW and a free-running linewidth of about 0.5 MHz. After a Faraday isolator, the beam goes through an electro-optic modulator (EOM). The EOM puts 50 MHz phase modulation on the input beam, which is used to lock the laser to the high-finesse

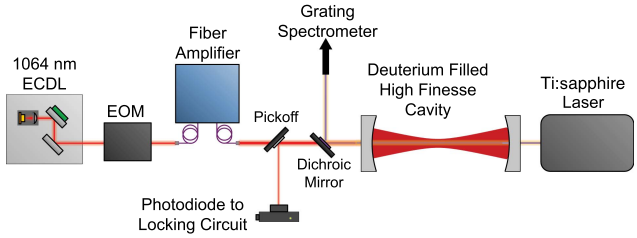

Fig. 1. Simplified schematic of the experiment. We prepare the Raman-based optical modulator by locking a high-power pump beam at a wavelength of 1064 nm to one of the longitudinal modes of the cavity. The high-power pump is produced by seeding an ytterbium-doped fiber amplifier with a custom-built external cavity diode laser (ECDL). With the pump locked to the cavity, the vibrational Stokes beam at a wavelength of 1.56 μm is generated through Raman lasing. The intense pump and Stokes laser beams in the cavity prepare a large molecular coherence. With the coherence prepared, the femtosecond Ti:sapphire oscillator passes through the cavity and gets modulated in a single pass (the cavity mirrors do not have high reflectivity near the Ti:sapphire wavelength of 800 nm). The modulated output is separated from the intense pump and Stokes lasers using a dichroic mirror and is analyzed using a grating-based spectrometer.

cavity. We then amplify the beam to a CW power of 20 W with an ytterbium fiber amplifier. When we lock the pump laser to the cavity, we observe CW Raman lasing of the Stokes beam. The Raman lasing occurs on the $|\nu=0,J=0\rangle \rightarrow |\nu=1,J=0\rangle$ fundamental vibrational transition of D_2 at a transition frequency of 90 THz (2994 cm^{-1}). The pump beam at a wavelength of 1.064 μm produces the Stokes beam at a wavelength of 1.56 μm. The intense pump and Stokes beams inside the cavity drive the molecular coherence and generate the anti-Stokes beam at a wavelength of 807 nm through four-wave mixing. The cavity mirrors do not have a high reflectivity at 807 nm, and the anti-Stokes light is generated through a single pass. At the cavity output, we typically observe ∼30 mW of pump, ∼20 mW of Stokes, and ∼0.1 mW of anti-Stokes light.

As mentioned above, we modulate a Ti:sapphire laser using the molecules driven by the intense pump and Stokes lasers. The Ti:sapphire laser cavity is in a z configuration with a dispersion-compensating prism pair and uses Kerr lensing for mode locking. We pump the Ti:sapphire crystal using a diode-pumped, frequency-doubled solid-state Nd:YAG laser with an optical power of 4 W in the green. The Ti:sapphire oscillator produces a train of pulses at the output with a pulse width of 50 fs, a repetition rate of 94 MHz, and an average power of 200 mW. After beam shaping and polarization control, the Ti:sapphire output is mode matched to the cavity and is modulated in a single pass. The cavity output is separated from the intense pump and Stokes beams using a dichroic mirror, and then sent into a custom-built grating-based spectrometer. The spectrometer uses a metal-coated grating with 1800 lines/mm and achieves ∼1 nm spectral resolution with a light sensitivity of ∼10 picowatts (per 1 nm spectral bin). Figure 2 shows the modulated Ti:sapphire output observed on the grating spectrometer over the 600–900 nm spectral

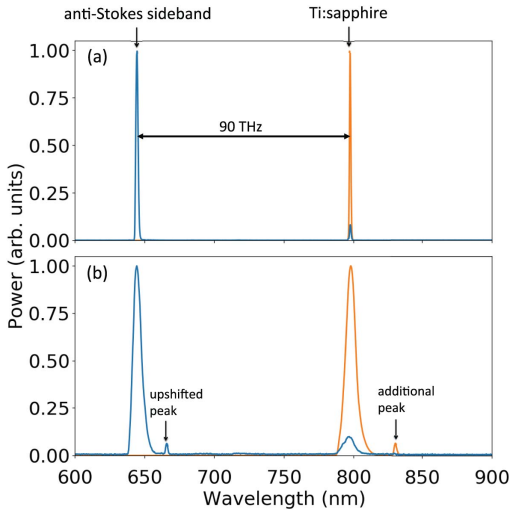

Fig. 2. Modulated Ti:sapphire spectrum at the output of the cavity as recorded on the grating spectrometer, clearly showing the incident Ti:sapphire spectrum as well as the frequency upshifted anti-Stokes sideband. The plots are obtained for two different modes of operation for the Ti:sapphire laser: (a) without mode locking (and therefore narrow spectrum) and (b) with mode locking. The solid blue lines are the spectrum analyzer scans showing the Ti:sapphire and the frequency upshifted spectrum simultaneously. The solid orange lines are separate scans of the initial unmodulated Ti:sapphire spectrum that are normalized in order to more clearly display the input spectral features.

range, clearly showing the frequency upshifted anti-Stokes sideband. Unfortunately, the Stokes sideband is at a wavelength of 1.04 μm and is blocked by the output cavity mirror due to high reflectance at this wavelength. The plots show the modulated output with the Ti:sapphire laser in two different modes of operation: (a) without mode locking (and therefore narrow spectral width) and (b) with mode locking. For both of these cases, the initial Ti:sapphire spectrum is replicated to the anti-Stokes sideband. This replication is especially clear in (b) where an additional spectral feature is also modulated and replicated in the upshifted spectrum. In these plots, the solid blue lines are the spectrum analyzer scans showing the Ti:sapphire and the frequency upshifted spectrum simultaneously. To avoid saturation of the spectrometer, a number of interference filters are used to attenuate the input Ti:sapphire spectrum. The solid orange lines are separate scans of the initial unmodulated Ti:sapphire spectrum that are normalized in order to more clearly display the input spectral features.

We note that the results of Fig. 2 have immediate important implications for ultrafast waveform synthesis. Our previous work showed the absolute linewidth of the molecular oscillations to be quite narrow, at the 10 kHz level [20]. As a result, the modulated output should retain the coherence properties of the incident beam. If a commercially available broadband Ti:sapphire femtosecond oscillator is used as the input carrier beam (10 fs pulse width, 700–900 nm spectral range), the modulated spectrum at the output would completely cover the 550–1250 nm spectral range, with the capability to produce sub-cycle 2-fs-long pulses.

The frequency upshifted anti-Stokes spectrum centered at 650 nm should retain the discrete-mode spectral nature of the initial Ti:sapphire oscillator. Specifically, for mode-locked operation, the anti-Stokes spectrum should synthesize a periodic train of pulses in the time domain at the Ti:sapphire laser repetition rate. Figure 3 shows this result. Here, we measure the full anti-Stokes light in the time domain using a fast photodiode and record the output on an electronic spectrum analyzer. As expected, the signal shows a strong narrow beat at the Ti:sapphire repetition rate of 94 MHz, demonstrating the discrete-mode nature of the anti-Stokes spectrum.

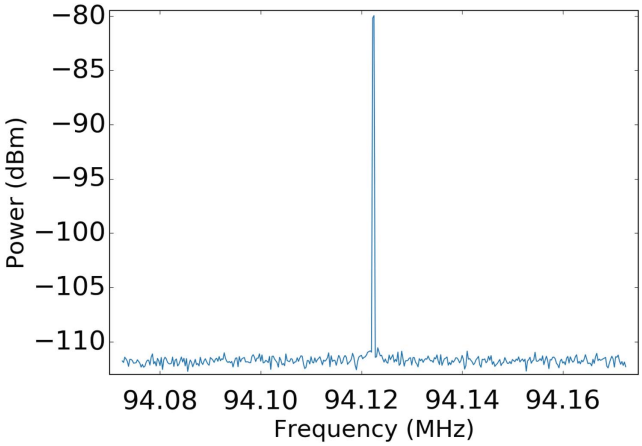

Fig. 3. Signal on an electronic spectrum analyzer from the anti-Stokes portion of the spectrum (centered at 650 nm) when detected on a fast photodiode. Due to the discrete-mode nature of the spectrum, there is a strong beat at 94.12 MHz. Within our measurement accuracy, this value coincides with the measured repetition rate of the Ti:sapphire oscillator.

Figure 4 shows the power conversion efficiency from the incident Ti:sapphire beam to the generated anti-Stokes sideband as the pressure in the chamber is increased. We observe an efficiency of $\sim 1 \times 10^{-6}$ for D_2 pressures in the range of 1–1.5 atm, with substantially reduced efficiency for higher pressures. This curve is largely determined by the locking performance of the high-power pump laser beam to the cavity and is not representative of the physics of Raman lasing. We have found that as the Stokes beam builds up from noise, the Raman lasing dynamics and thermal effects on the mirrors significantly degrade the lock performance, especially at higher pressures. If these challenges can be overcome in the future, substantially larger steady-state CW modulation efficiencies will likely be achievable.

We have verified that the current limitation to steady-state conversion is locking performance by investigating modulation in the transient regime. The lock to the cavity has two feedback loops: one to the ECDL current (fast corrections) and the other one to the cavity piezo (slow corrections). To investigate modulation in the transient regime, we turn off the feedback loops and look at modulation as the cavity length is scanned using the piezo-producing resonance peaks spaced by the free spectral range. Figure 5 shows the pump (1.06 μm), the Stokes (1.56 μm), and the anti-Stokes (807 nm) pulses recorded on fast photodiodes at the output of the cavity as the cavity length is scanned through three spectral ranges. The Stokes Raman lasing is confined mostly to the peak of the pump laser build-up, which then produces more sharply peaked anti-Stokes light due to the nonlinear nature of generation. The fluctuations in the pump laser scan are likely a result of the laser frequency jitter and mechanical perturbations to the cavity occurring during the time scales of the scan. Using averaging over many scans, we smooth out these fluctuations. We then

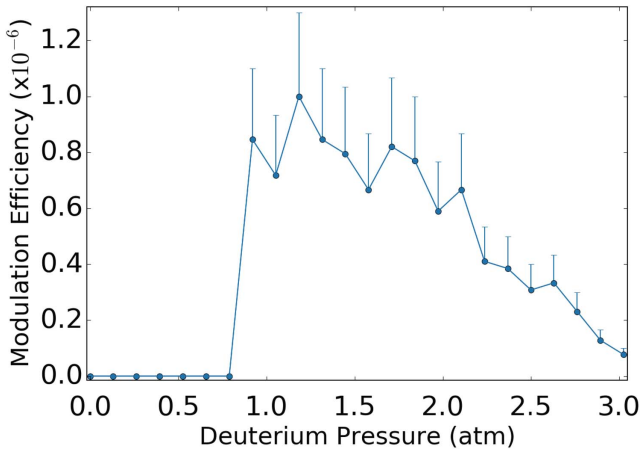

Fig. 4. Modulation efficiency as a function of D_2 pressure in the chamber. We observe an efficiency of $\sim 1 \times 10^{-6}$ for D_2 pressures in the range of 1–1.5 atm, with substantially reduced efficiency for higher pressures. This curve is largely determined by the locking performance of the high-power pump laser beam to the cavity and is not representative of the physics of Raman lasing. At each pressure, the data points are the observed modulation efficiency obtained after about 1 h of tuning. Typically, with extended tuning at a given pressure, we can improve the efficiency by about 30%. To reflect this, the error bars are one-sided with large uncertainty only in the upward direction.

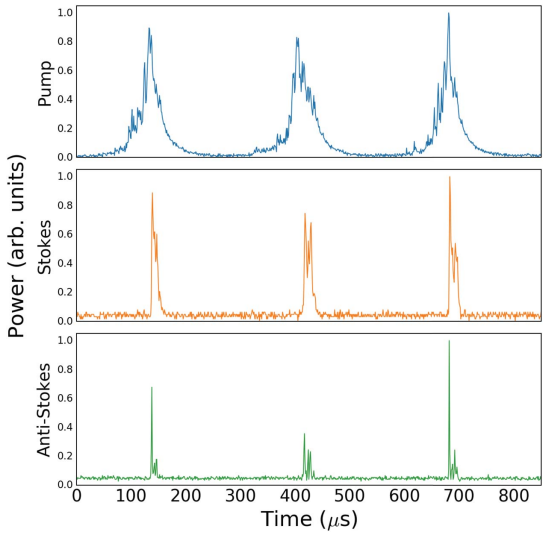

Fig. 5. Pump (1.06 μm), the Stokes (1.56 μm), and the anti-Stokes (807 nm) pulses recorded on fast photodiodes as the cavity length is scanned through three spectral ranges. The Stokes Raman lasing is confined mostly to the peak of the pump laser build-up, which then produces more sharply peaked anti-Stokes light due to the nonlinear nature of generation. The anti-Stokes light is generated in a single pass through the cavity, since the mirrors do not have high reflectivity at this wavelength. Using the peak-generated anti-Stokes power, we infer that the single-pass efficiency of our modulator reaches a peak value of $\sim 10^{-4}$.

estimate the peak-power values for each beam inside the cavity using known transmittance of the output mirror. By dividing the peak power of the anti-Stokes beam to the peak power of the pump beam, we infer that the single-pass efficiency of our modulator reaches a value of $\sim 10^{-4}$ in the transient regime, which is about two orders of magnitude higher than the steady-state modulation efficiencies of Fig. 4. The dephasing rate of the Raman transition at a pressure of 1 atm is 171 MHz. Using this dephasing rate, we calculate the saturation time for the Raman transition to be much longer compared to the diffusion time of the molecules out of the beam path, which is calculated to be 1.1 ms. As a result, the increase in modulation efficiency is not due to reduced saturation, but rather due to an increase in the intracavity pump and Stokes intensities in the transient regime.

In conclusion, we have described a new method to broaden the frequency spectrum of a femtosecond oscillator. The method relies on CW molecular modulation using molecules driven to a highly coherent state with intense pump and Stokes lasers inside a high-finesse cavity. As mentioned above, one key application of our experiment is to ultrafast waveform synthesis. Using our method, a broadband Ti:sapphire laser at the input will produce a spectrum covering more than an octave bandwidth at the output, with the capability to synthesize sub-cycle pulses. A more practical and device-oriented application of this work is to the construction of ultrafast optical modulators. Optical modulators have traditionally utilized electro-optic or acousto-optic effects in crystals, and have achieved modulation rates as high as 200 GHz with efficiencies at the 10^{-4} level [22]. Faster modulators with THz-level modulation rates can be constructed using an all-optical approach, but these are typically narrowband, have low modulation efficiency, or utilize pulsed lasers with significant limitations [23–25]. One promising future extension of our approach is to utilize Raman transitions in glass microspheres. Whispering gallery modes of glass microspheres can have very high finesse, and CW Raman lasing with low-pump-power thresholds has been observed [26]. Such systems may, in the future, allow constructing compact and efficient CW optical modulators with rates deep into the THz regime.

Funding. National Science Foundation (NSF) (1306898); Wisconsin Alumni Research Foundation (WARF).

Acknowledgment. We thank Zach Buckholtz, Ben Lemberger, and Dipto Das for many helpful discussions. We are also grateful to Dick Prepost for the loan of the Ti:sapphire oscillator.

REFERENCES

1. T. Brabec and F. Krausz, Rev. Mod. Phys. **72**, 545 (2000).
2. T. W. Hansch and H. Walther, Rev. Mod. Phys. **71**, S242 (1999).
3. R. W. J. Ranka and A. Stentz, Opt. Lett. **25**, 25 (2000).
4. S. A. Diddams, D. J. Jones, L. S. Ma, S. T. Cundiff, and J. L. Hall, Opt. Lett. **25**, 186 (2000).
5. S. Yoshikawa and T. Imasaka, Opt. Commun. **96**, 94 (1993).
6. H. Kawano, Y. Hirakawa, and T. Imasaka, IEEE J. Quantum Electron. **34**, 260 (1998).
7. A. V. Sokolov, D. R. Walker, D. D. Yavuz, G. Y. Yin, and S. E. Harris, Phys. Rev. Lett. **85**, 562 (2000).
8. A. V. Sokolov, M. Y. Shverdin, D. R. Walker, D. D. Yavuz, A. M. Burzo, G. Y. Yin, and S. E. Harris, J. Mod. Opt. **52**, 285 (2005).
9. J. Q. Liang, M. Katsuragawa, F. Le Kien, and K. Hakuta, Phys. Rev. Lett. **85**, 2474 (2000).
10. M. Katsuragawa, J. Q. Liang, F. Le Kien, and K. Hakuta, Phys. Rev. A **65**, 025801 (2002).
11. J. K. Brasseur, K. S. Repasky, and J. L. Carlsten, Opt. Lett. **23**, 367 (1998).
12. J. K. Brasseur, P. A. Roos, K. S. Repasky, and J. L. Carlsten, J. Opt. Soc. Am. B **16**, 1305 (1999).
13. H. S. Chan, Z. M. Hsieh, W. H. Liang, A. H. Kung, C. K. Lee, C. J. Lai, R. P. Pan, and L. H. Peng, Science **331**, 1165 (2011).
14. C. H. Lu, L. F. Yang, M. Zhi, A. V. Sokolov, S. D. Yang, C. C. Hsu, and A. H. Kung, Opt. Express **22**, 4075 (2014).
15. M. Zhi, K. Wang, X. Hua, H. Schuessler, J. Strohaber, and A. V. Sokolov, Opt. Express **21**, 27750 (2013).
16. K. Yoshii, J. K. Anthony, and M. Katsuragawa, Light Sci. Appl. **2**, e58 (2013).
17. M. Katsuragawa and K. Yoshii, Phys. Rev. A **95**, 033846 (2017).
18. F. L. Kien, S. N. Hong, and K. Hakuta, Phys. Rev. A **64**, 051803 (2001).
19. S. Gundry, M. P. Anscombe, A. M. Abdulla, E. Sali, J. W. G. Tisch, P. Kinsler, G. H. C. New, and J. P. Marangos, Opt. Lett. **30**, 180 (2005).
20. J. J. Weber and D. D. Yavuz, Opt. Lett. **38**, 2449 (2013).
21. D. C. Gold, J. J. Weber, and D. D. Yavuz, Appl. Sci. **4**, 498 (2014).
22. M. Chacinski, U. Westergren, B. Stoltz, L. Thylen, R. Schatz, and S. Hammerfeldt, J. Lightwave Technol. **27**, 3410 (2009).
23. M. Hochberg, T. Baehr-Jones, G. Wang, M. Shearn, K. Harvard, J. Luo, B. Chen, Z. Shi, R. Lawson, P. Sullivan, A. K. Y. Jen, L. Dalton, and A. Scherer, Nat. Mater. **5**, 703 (2006).
24. X. Fang, M. L. Tseng, J. Ou, K. F. MacDonald, D. P. Tsai, and N. I. Zheludev, Appl. Phys. Lett. **104**, 141102 (2014).
25. W. Li, B. Chen, C. Meng, W. Fang, Y. Xiao, X. Li, Z. Hu, Y. Xu, L. Tong, H. Wang, W. Liu, J. Bao, and Y. R. Shen, Nano Lett. **14**, 955 (2014).
26. I. S. Grudinin and S. Maleki, J. Opt. Soc. Am. B **25**, 594 (2008).